US007847669B2

(12) **United States Patent**
Ayazi et al.

(10) **Patent No.: US 7,847,669 B2**
(45) **Date of Patent: Dec. 7, 2010**

(54) **MICRO-ELECTROMECHANICAL SWITCHED TUNABLE INDUCTOR**

(75) Inventors: **Farrokh Ayazi**, Atlanta, GA (US); **Mina Raieszadeh**, Atlanta, GA (US); **Paul A. Kohl**, Atlanta, GA (US)

(73) Assignee: **Georgia Tech Research Corporation**, Atlanta, GA (US)

(*) Notice: Subject to any disclaimer, the term of this patent is extended or adjusted under 35 U.S.C. 154(b) by 28 days.

(21) Appl. No.: **11/999,527**

(22) Filed: **Dec. 6, 2007**

(65) **Prior Publication Data**

US 2008/0136572 A1 Jun. 12, 2008

Related U.S. Application Data

(60) Provisional application No. 60/868,810, filed on Dec. 6, 2006.

(51) **Int. Cl.**
H01F 5/00 (2006.01)
H01F 27/28 (2006.01)
H01F 21/02 (2006.01)
H01F 21/10 (2006.01)
H01G 2/00 (2006.01)
H01G 5/00 (2006.01)

(52) **U.S. Cl.** **336/200**; 336/223; 336/232; 336/146; 336/222; 336/87; 361/272; 361/287

(58) **Field of Classification Search** .... None
See application file for complete search history.

(56) **References Cited**

U.S. PATENT DOCUMENTS

4,249,262 A * 2/1981 Fenk 455/333
5,578,976 A * 11/1996 Yao 333/262
5,872,489 A * 2/1999 Chang et al. 331/179
5,959,516 A * 9/1999 Chang et al. 334/14
6,232,847 B1 * 5/2001 Marcy et al. 331/167
6,549,096 B2 4/2003 Groves et al.

(Continued)

OTHER PUBLICATIONS

James Salvia et al, "Tunable on-Chip Inductors up to 5 GHz using patterned permalloy Laminations,"Dec. 2005 IEEE IEDM, pp. 943-946.
Shih et al, "Tunable solenoid microinductors utilizing Permalloy electro-thermal vibromotors," Sep. 2004 IEEE MEMS, pp. 793-796.

(Continued)

Primary Examiner—Elvin G Enad
Assistant Examiner—Mangtin Lian
(74) *Attorney, Agent, or Firm*—Thomas, Kayden, Horstemeyer & Risley, LLP

(57) **ABSTRACT**

Disclosed is an integrated tunable inductor having mutual micromachined inductances fabricated in close proximity to a tunable inductor that is switched in and out by micromechanical ohmic switches to change the inductance of the integrated tunable inductor. To achieve a large tuning range and high quality factor, silver is preferably used as the structural material to co-fabricate the inductors and micromachined switches, and silicon is selectively removed from the backside of the substrate. Using this method, exemplary tuning of 47% at 6 GHz is achievable for a 1.1 nH silver inductor fabricated on a low-loss polymer membrane. The effect of the quality factor on the tuning characteristic of the integrated inductor is evaluated by comparing the measured result of substantially identical inductors fabricated on various substrates. To maintain the quality factor of the silver inductor, the device may be encapsulated using a low-cost wafer-level polymer packaging technique.

22 Claims, 8 Drawing Sheets

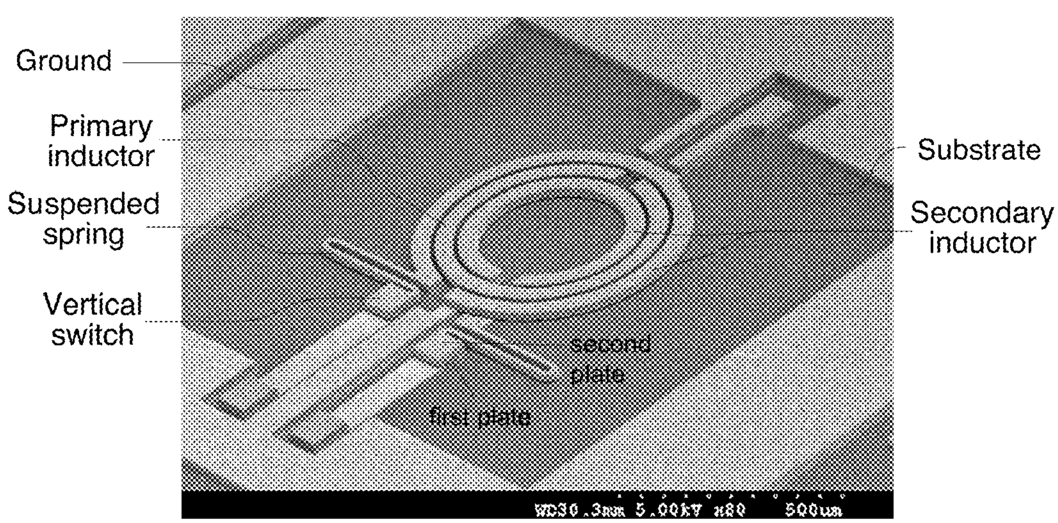

U.S. PATENT DOCUMENTS

6,573,822	B2 *	6/2003	Ma et al.	336/223
6,768,628	B2 *	7/2004	Harris et al.	361/277
6,800,912	B2 *	10/2004	Ozgur	257/414
6,977,569	B2 *	12/2005	Deligianni et al.	335/78
7,042,319	B2 *	5/2006	Ishiwata et al.	335/78
7,091,784	B1	8/2006	Terrovitis	
7,598,838	B2 *	10/2009	Hargrove et al.	336/200
2002/0190835	A1 *	12/2002	Ma et al.	336/223
2003/0030527	A1 *	2/2003	Mhani et al.	336/130
2003/0060051	A1 *	3/2003	Kretschmann et al.	438/694
2003/0099082	A1 *	5/2003	Tuo et al.	361/290
2003/0122207	A1 *	7/2003	Yen et al.	257/421
2004/0100341	A1 *	5/2004	Luetzelschwab et al.	333/32
2005/0068146	A1 *	3/2005	Jessie	336/200
2006/0115919	A1 *	6/2006	Gogoi et al.	438/50
2006/0290450	A1 *	12/2006	Weller et al.	333/262
2006/0290457	A1 *	12/2006	Lee et al.	336/200
2007/0273013	A1 *	11/2007	Kohl et al.	257/682

OTHER PUBLICATIONS

C. M. Tassetti et al., “Tunable RF MEMS microinductors for future communication systems,” Sep. 2003 IEEE MTT-S, vol. 3, pp. 541-545.

I. Zine-El-Abidine et al., “RF MEMS tunable inductor,” 2004 IEEE Microwaves, Radar and Wireless Corn., vol. 3, pp. 817-819, May 2004.

P. Monajemi et al, “A Low-cost Wafer-level Packaging Technology,” 2005 IEEE MEMS, Jan. 2005, pp. 634-637.

M. Rais-Zadeh et al, “High-Q Micromachined Silver Passives and Filters,” accepted to IEEE IEDM, Dec. 2006.

M. Rais-Zadeh et al., “Characterization of high-Q sprial inductors on thick insulator-on-silicon” J. of Micromechanics and Microengineering (Sep. 2005) vol. 15 pp. 2105-2112.

M. Raieszadeh et al., “High-Q integrated inductors on trenched Si islands” Proc. of IEEE MEMS Conf. (Jan. 2005) pp. 199-202.

R. Manepalli et al., “Silver metallization for advanced interconnects” IEEE Trans. Advanced Packaging (Feb. 1999) vol. 22 No. 1 pp. 4-8.

* cited by examiner

Fig. 1

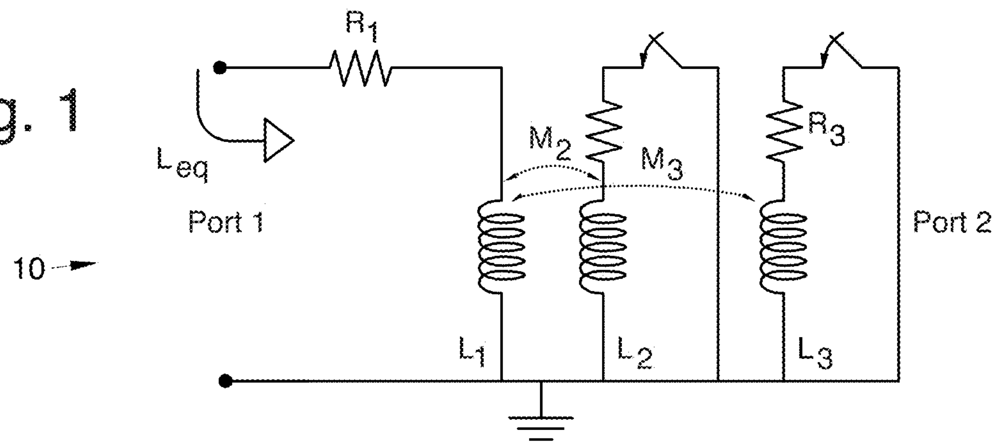

Fig. 2

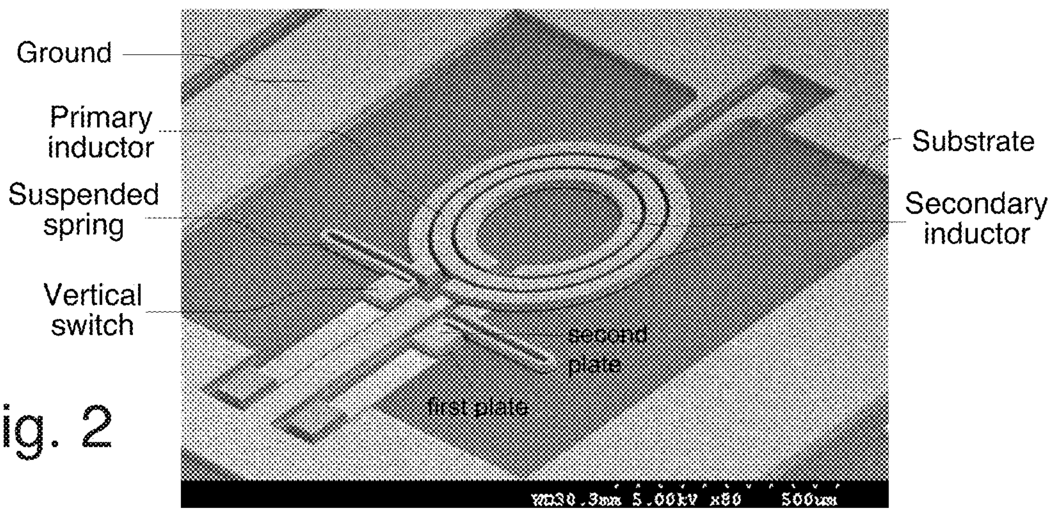

Fig. 3

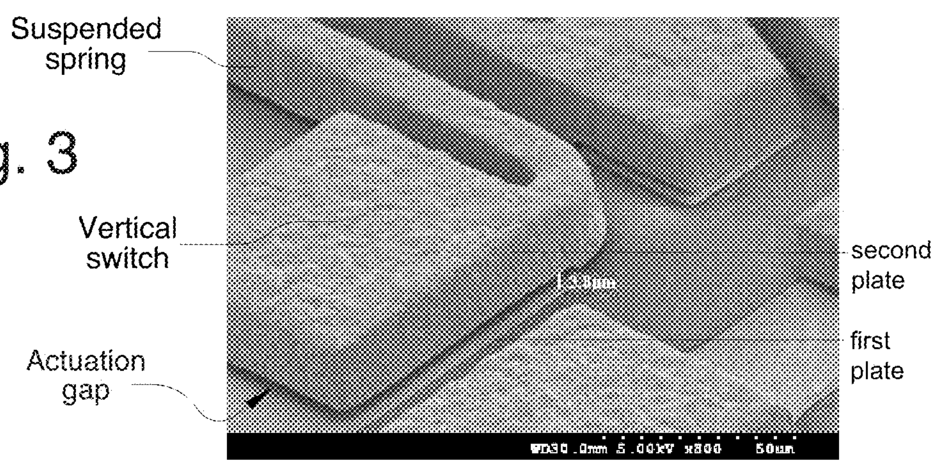

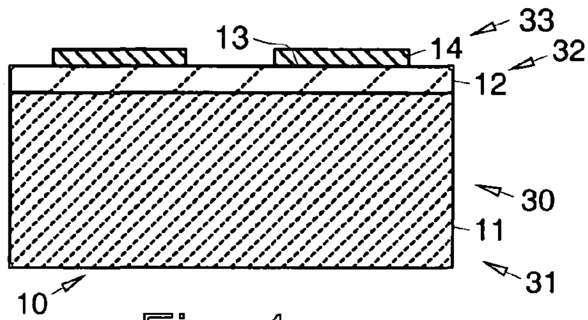

Fig. 4a

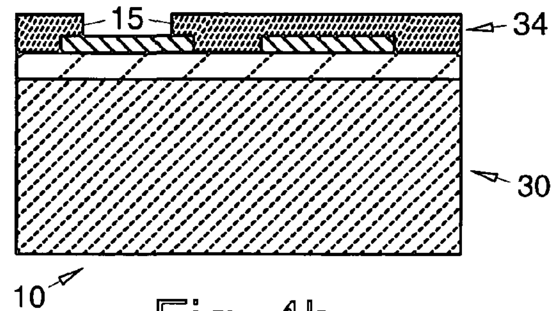

Fig. 4b

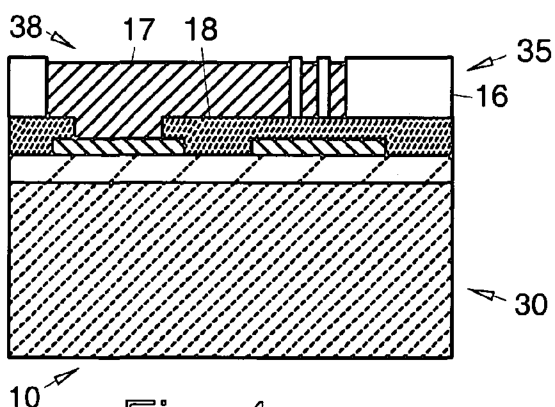

Fig. 4c

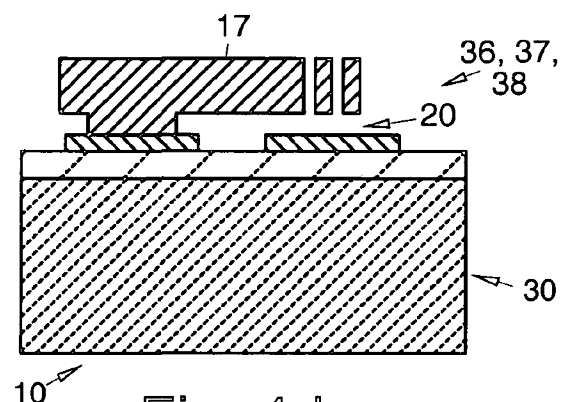

Fig. 4d

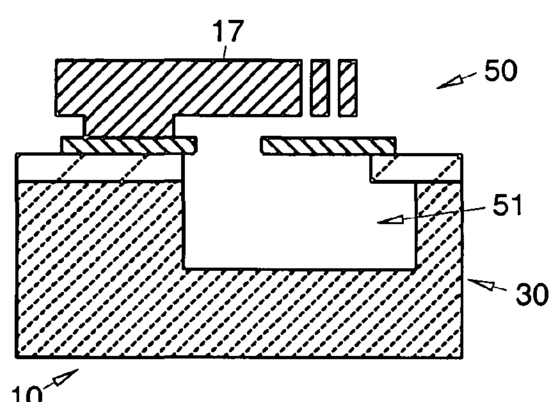

Fig. 4d'

Fig. 4e

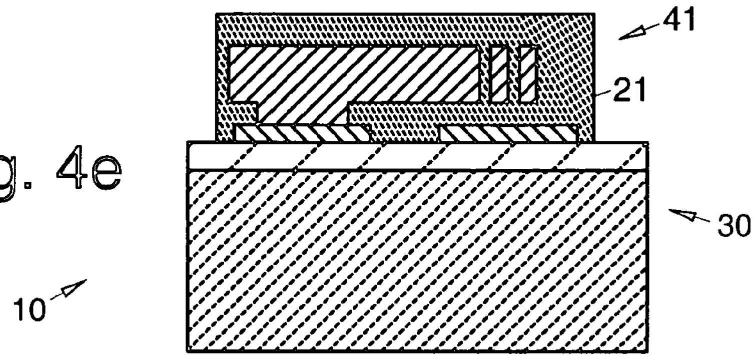

Fig. 4f

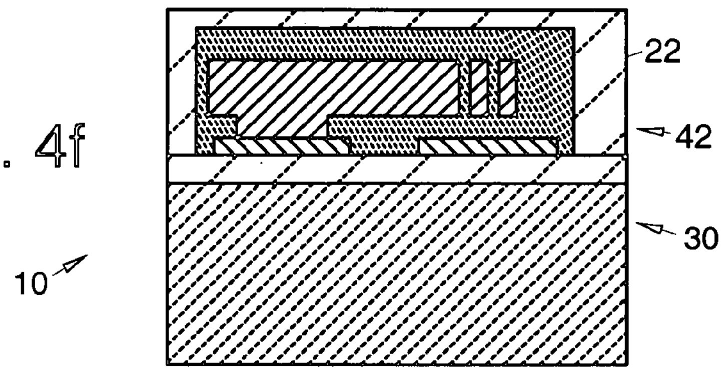

Fig. 4g

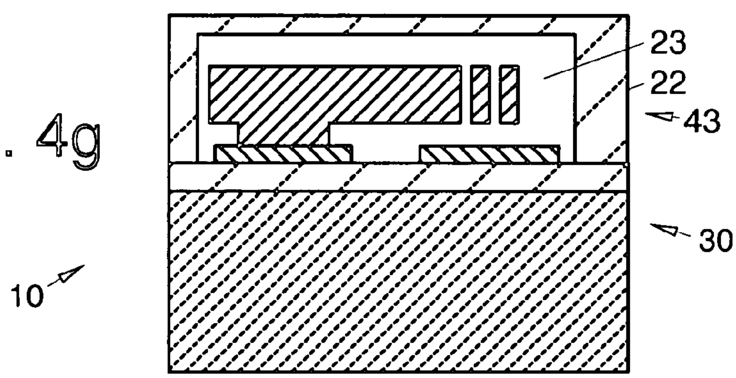

Fig. 4h

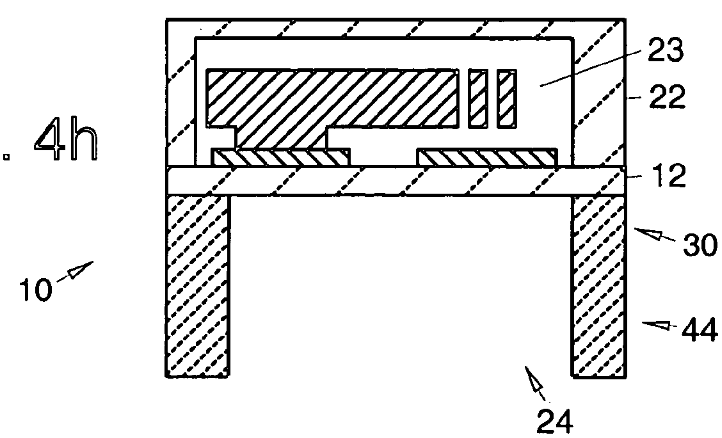

Fig. 5

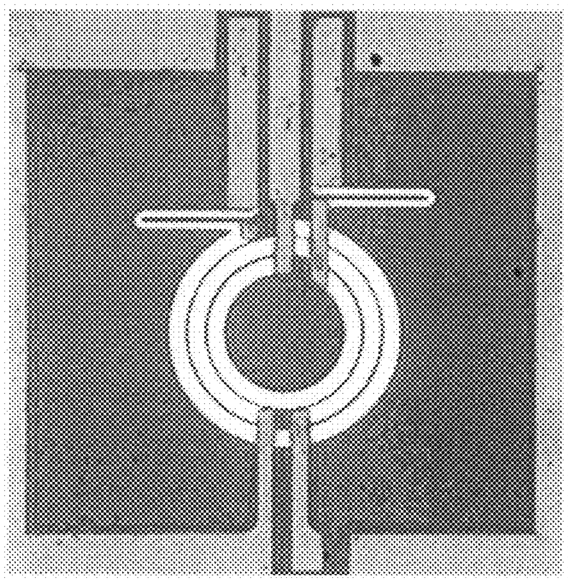

Fig. 6a

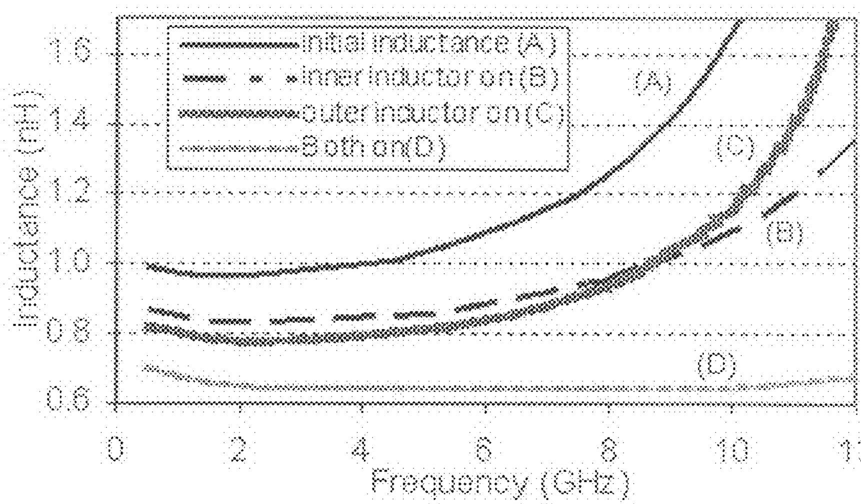

Fig. 6b

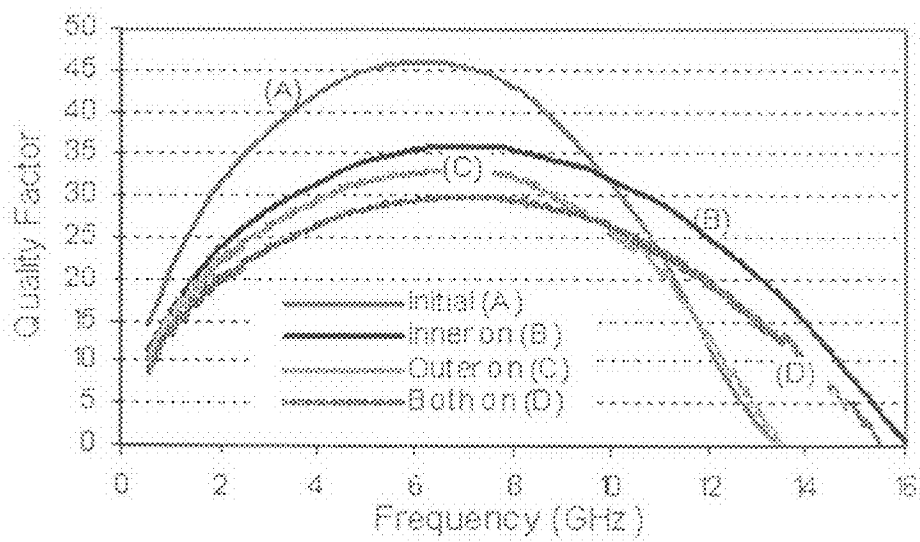

Fig. 7

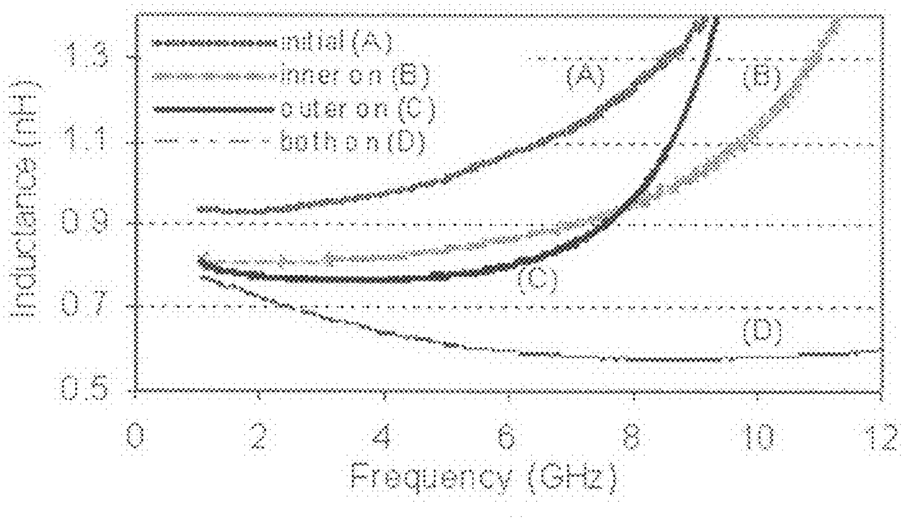

Fig. 8

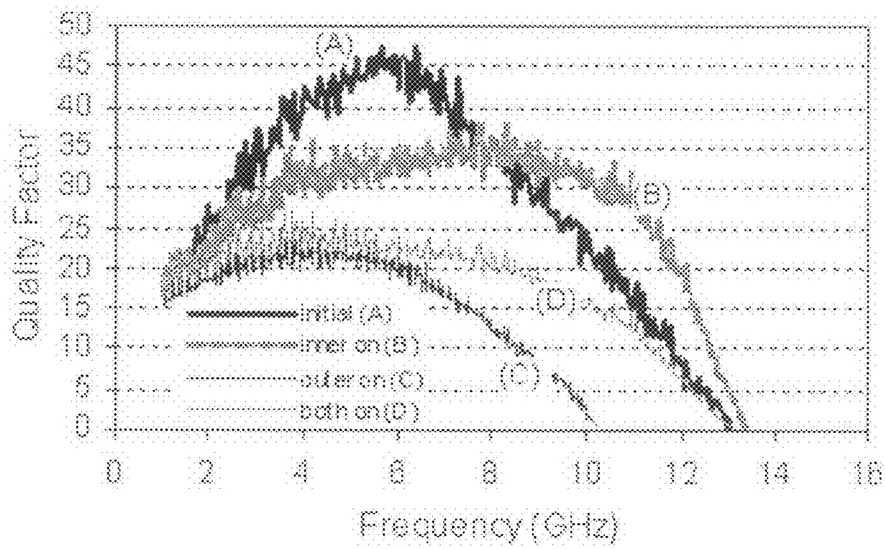

Fig. 9

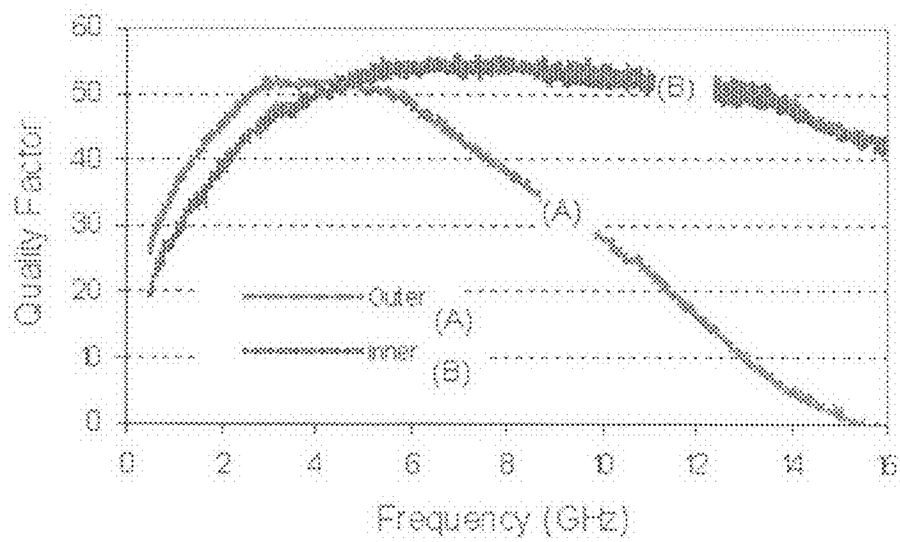

Fig. 10a

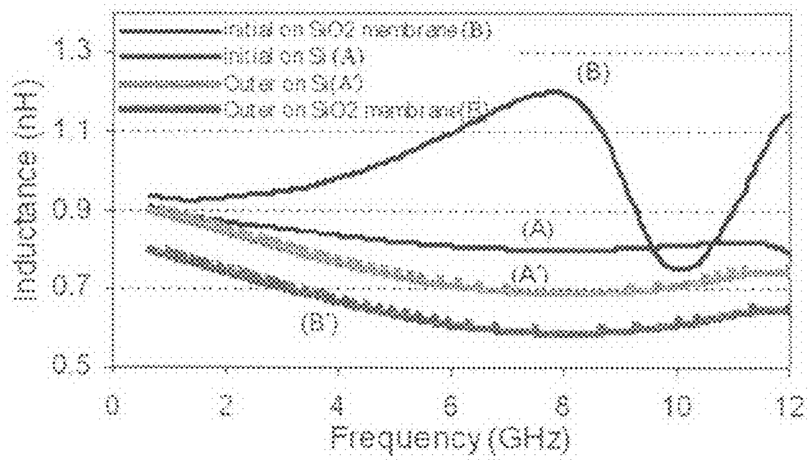

Fig. 10b

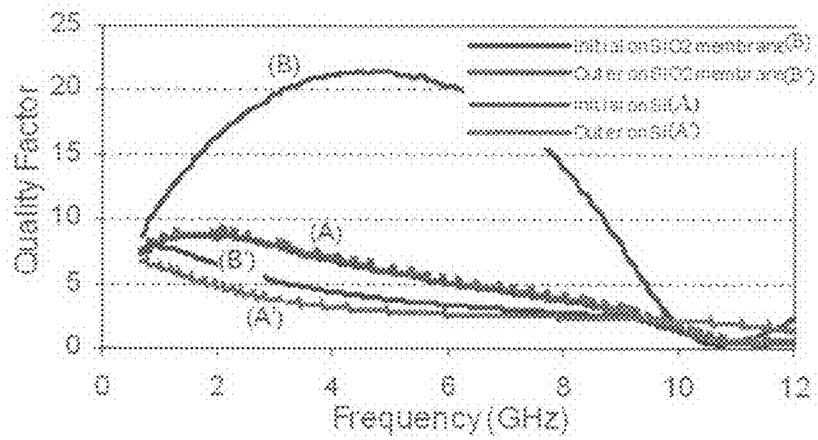

Fig. 11a

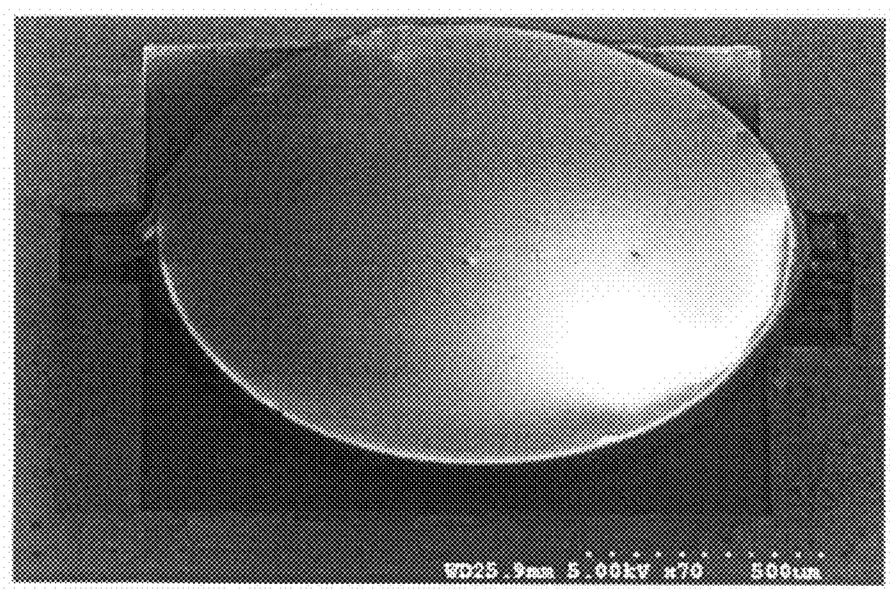

Fig. 11b

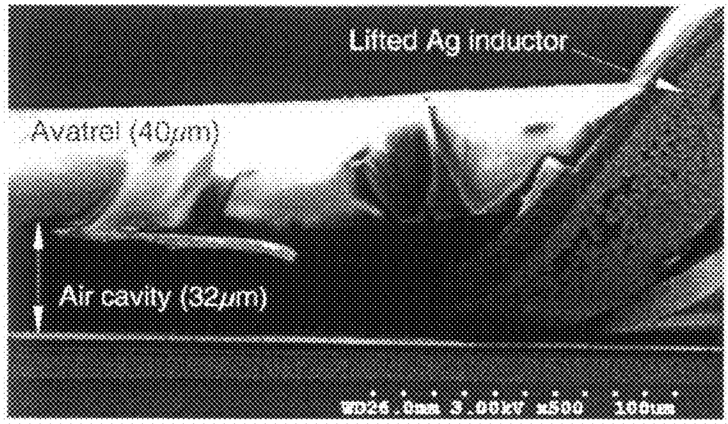

Fig. 12

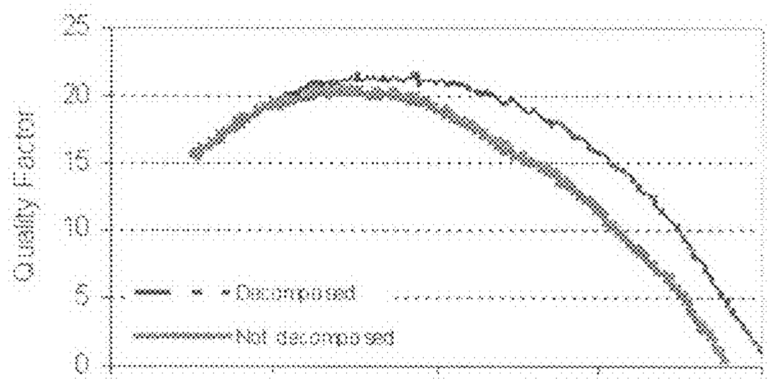

Fig. 13

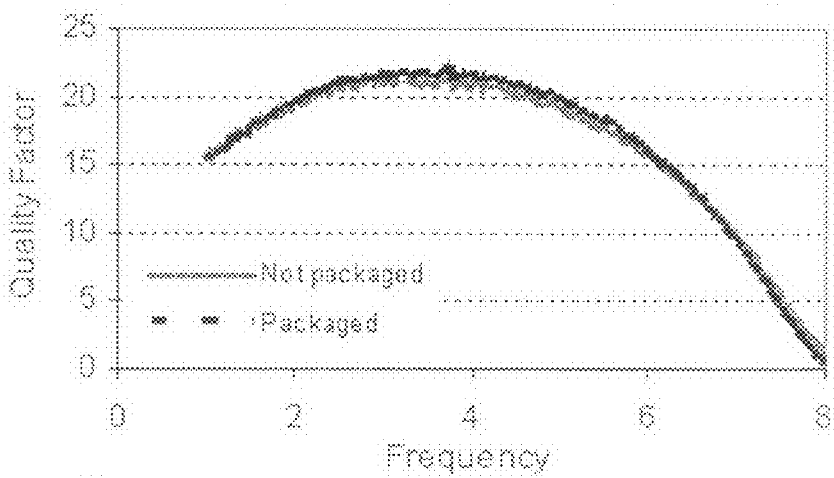

Fig. 14

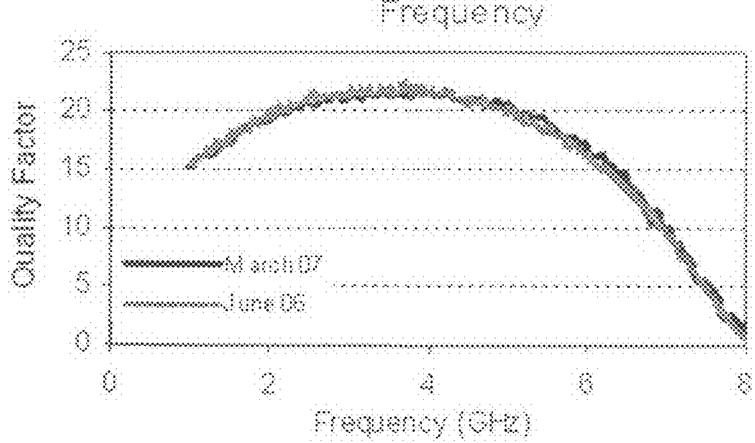

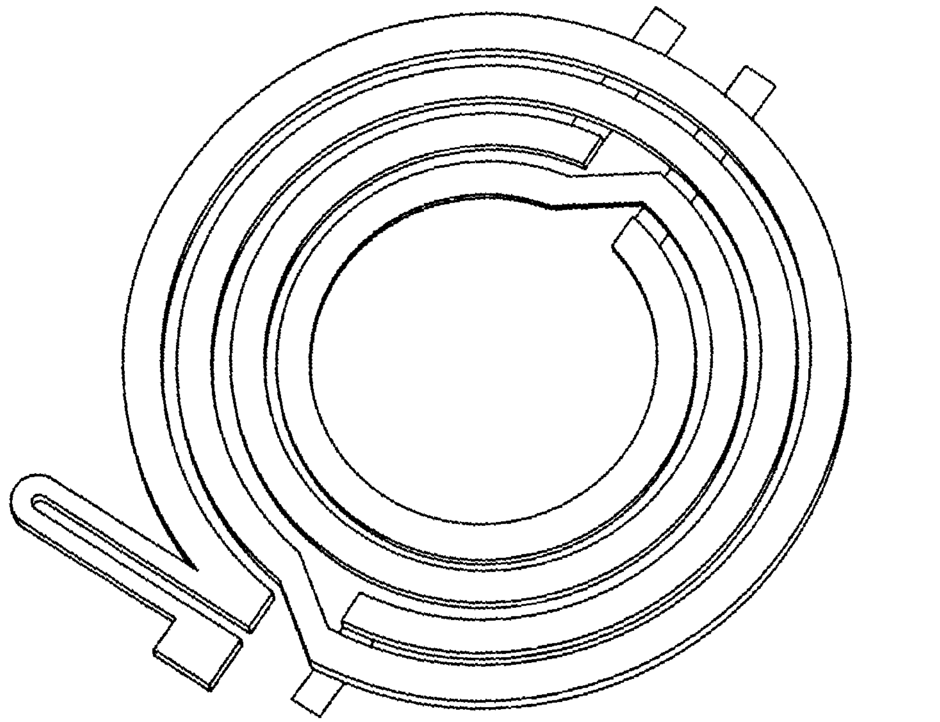

Fig. 15a

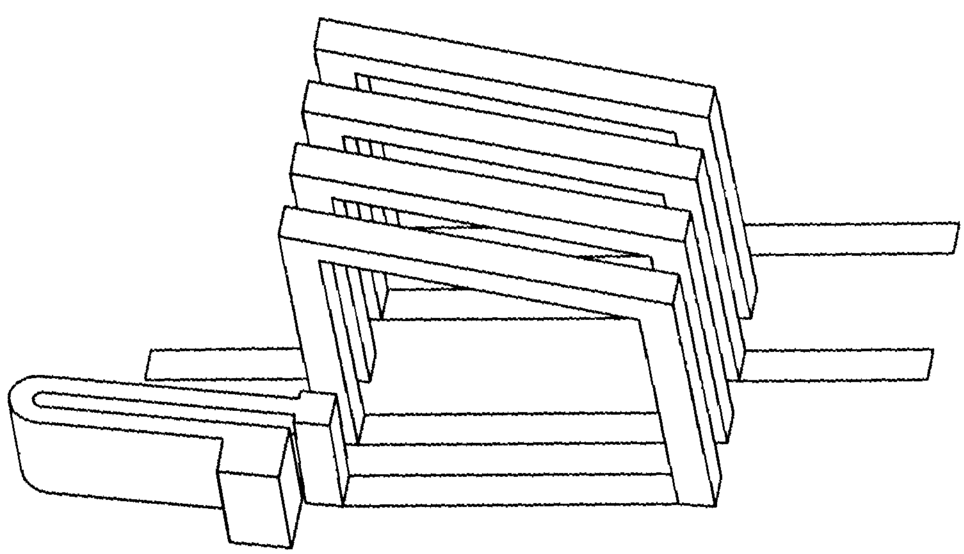

Fig. 15b

MICRO-ELECTROMECHANICAL SWITCHED TUNABLE INDUCTOR

CROSS REFERENCE TO RELATED APPLICATIONS

This application claims priority to U.S. provisional application entitled "Micromachined Switched Tunable Inductor" having Ser. No. 60/868,810, filed Dec. 6, 2006.

STATEMENT REGARDING FEDERALLY SPONSORED RESEARCH OR DEVELOPMENT

This invention was made with government support under agreement ECS-0348286 awarded by the National Science Foundation. The Government has certain rights in the invention.

BACKGROUND

The present invention relates generally to tunable inductors, and more particularly, to microelectromechanical systems (MEMS) switched tunable inductors.

Tunable inductors can find application in frequency-agile radios, tunable filters, voltage controlled oscillators, and reconfigurable impedance matching networks. The need for tunable inductors becomes more critical when optimum tuning or impedance matching in a broad frequency range is desired. Both discrete and continuous tuning of passive inductors using micromachining techniques have been reported in the literature.

Discrete tuning of inductors is usually achieved by changing the length or configuration of a transmission line using micromachined switches. The incorporation of switches in the body of the tunable inductor increases the resistive loss and hence reduces the quality factor (Q). Alternatively, continuous tuning of inductors may be realized by displacing a magnetic core, changing the permeability of the core, or using movable structures with large traveling range. Although significant tuning has been reported using these methods, the fabrication or the actuation techniques are complex, making the on-chip implementation of the tunable inductors difficult. In addition, Q of the reported tunable inductors is not sufficiently high for many wireless and RF integrated circuit applications.

Therefore, there is a need for high-performance small form-factor tunable inductors. Also, to overcome the shortcomings of prior art tunable inductors, an improved design and micro-fabrication method for tunable inductors is necessary.

BRIEF DESCRIPTION OF THE DRAWINGS

The various features and advantages of the present invention may be more readily understood with reference to the following detailed description taken in conjunction with the accompanying drawings, wherein like reference numerals designate like structural elements, and in which:

FIG. **1** illustrates an electrical model of an exemplary switched tunable inductor;

FIG. **2** is a SEM view of a 20 μm thick silver switched tunable inductor fabricated on an Avatrel™ polymer membrane;

FIG. **3** is a close-up SEM view of the switch, showing the actuation gap;

FIGS. **4***a-h* illustrate an exemplary method for fabricating a packaged switched tunable inductor;

FIG. **5** is a micrograph of the switched silver inductor taken from the backside of the Avatrel™ membrane;

FIG. **6***a* and **6***b* are graphs that illustrate simulated inductance and Q of a switched tunable inductor on Avatrel™ membrane, respectively, showing a maximum tuning of 47.5% at 6 GHz;

FIG. **7** illustrates measured inductance showing a maximum tuning of 47% at 6 GHz when both inductors are on;

FIG. **8** illustrates measured embedded Q showing the Q drops as the inductor is tuned;

FIG. **9** illustrates measured Q of the inductors at port two on Avatrel™ membrane;

FIG. **10***a* and **10***b* illustrate measured inductance and embedded Q, respectively, of substantially identical tunable inductors fabricated on passivated silicon substrate (A), and 20 μm thick silicon dioxide membrane;

FIG. **11***a* is a SEM view of an exemplary packaged switched inductor and FIG. **11***b* is a close-up SEM view of a package showing the air cavity inside;

FIG. **12** illustrates measured embedded Q of two substantially identical inductors, before decomposition, one packaged and one un-packaged;

FIG. **13** illustrates measured embedded Q of two substantially identical inductors when both switches are off, one packaged and one un-packaged;

FIG. **14** illustrates measured embedded Q of the packaged silver tunable inductor, showing no degradation in Q after about 10 months; and

FIGS. **15***a* and **15***b* illustrate exemplary multi-turn inductors in accordance with the current disclosure.

DETAILED DESCRIPTION

Disclosed are small form-factor high-Q switched tunable inductors **10** for use in a frequency range of about 1-10 GHz. In this frequency range, the permeability of most magnetic materials degrades, making them unsuitable for use at low RF frequencies. Also, small displacement is preferred to simplify the encapsulation process of the tunable inductors **10**. Tunable inductors **10** are disclosed based on transformer action using on-chip micromachined vertical switches with an actuation gap of a few micrometers. Silver (Ag) is preferably used since it has high electrical conductivity and low Young's modulus compared with other metals. To encapsulate the tunable inductors **10**, a wafer-level polymer packaging technique or method **30** (FIG. **4**) is employed. The fabrication method **30** is simple and requires only six lithography steps, including packaging steps, and is post-CMOS compatible. Using this method **30**, a reduced-to-practice 1.1 nH silver tunable inductor **10** is switched to four discrete values and shows a maximum tuning of 47% at 6 GHz. This inductor **10** exhibits an embedded Q in the range of 20 to 45 at 6 GHz and shows no degradation in Q after packaging. The disclosed switched tunable inductor **10** outperforms reported tunable inductors with respect to its high embedded quality factor at radio frequencies.

Design

FIG. **1** shows a schematic view of an exemplary switched tunable inductor **10**. The inductance is taken from port one, and a plurality of inductors at port two (secondary inductors) are switched in and out (two inductors in this case). Inductors may be one-turn or multi-turn having spiral or solenoid configurations and the switches are micromachined. Inductors at port two are different in size, and thus have a different mutual inductance effect on port one when activated. The effective inductance of port one can have $1+n(n+1)/2$ different states, where n is the number of inductors at port two. In the case of two inductors at port two, four discrete values can be achieved.

The equivalent inductance and series resistance seen from port one are found from

$$L_{eq} = L_1\left(1 - \sum_{i=2}^{n+1} \frac{b_i k_i^2 L_i^2 \omega^2}{R_i^2 + L_i^2 \omega^2}\right) \quad b_i = 0 \text{ or } 1 \tag{1}$$

$$R_{eq} = R_1 + \sum_{i=2}^{n+1} \frac{b_i R_i k_i^2 L_1 L_i \omega^2}{R_i^2 + L_i^2 \omega^2} \quad b_i = 0 \text{ or } 1 \tag{2}$$

where L_1 is the inductance at port one; L_i is the inductance value of the secondary inductors; R_i represents the series resistance of each secondary inductor plus the contact resistance of its corresponding switch; k_i is the coupling coefficient; b_i represents the state of the switch and is 1 (or 0) when the switch is on (or off), and ω is the angular frequency.

In equations (1) and (2), the parasitic capacitances are not considered. If the parasitic capacitances are taken into account, it can be shown that the equivalent inductance seen from port one when all of the switches at port two are open ($L_{eq(off\text{-}state)}$) is given by

$$L_{eq(off-state)} = L_1\left(1 + \sum_{i=1}^{n+1} k_i^2 \frac{1 - \frac{\omega^2}{\omega_{SRi}^2}}{\frac{\omega^2}{Q_i^2 \omega_{SRi}^2} - 2 + \frac{\omega^2}{\omega_{SRi}^2} + \frac{\omega_{SRi}^2}{\omega^2}}\right) \tag{3}$$

where $Q_i = L_i\omega/R_i$ is the quality factor of the secondary inductors; ω_{SRi} is defined as

$$\omega_{SRi} = \frac{1}{\sqrt{L_i(C_i + C_{swi})}} \tag{4}$$

where C_i denotes the self-capacitance of each inductor and C_{swi} is the off-state capacitance of its associated switch. If secondary inductors are high Q and have a resonance frequency much larger than the operating frequency ($\omega \ll \omega_{SRi}$), $L_{eq(off\text{-}state)}$ can be approximated by

$$L_{eq(off-state)} \overset{\omega \ll \omega_{SRi}}{\approx} L_1\left(1 + \sum_{i=1}^{n+1} k_i^2 \frac{\omega^2}{\omega_{SRi}^2 - 2\omega^2}\right) \approx L_1 \tag{5}$$

In this case, the largest change in the effective inductance occurs when all switches at port two are on and the percentage tuning can be found from

$$\%\ \text{tuning} = \sum_{i=2}^{n+1} \frac{b_i k_i^2 L_i^2 \omega^2}{(R_i^2 + L_i^2 \omega^2)} \times 100 \tag{6}$$

From equations (5) and (6) it can be seen that to achieve large tuning, R_i should be much smaller than the reactance of the secondary inductors ($L_i\omega$), which requires high-Q inductors and low-contact resistance switches that are best implemented using micromachining technology. For this reason, as disclosed herein, silver, which has the highest electrical conductivity of all materials at room temperature, is used to co-implement high-Q inductors and micromachined ohmic switches using a low-temperature fabrication process. The switches are actuated by applying a DC voltage to port two. The use of silver also offers the advantage of having a smaller tuning voltage compared to the other high conductivity metals (e.g., copper) because of its lower Young's modulus. However, it is to be understood that the disclosed switched tunable inductors can be made of other metals such as gold and/or copper at the expense of lower quality factor and smaller tuning range.

FIG. **2** shows a scanning electron microscope (SEM) view of a silver switched tunable inductor **10**. The inductors at port two are in series connection with a micromachined vertical ohmic switch through a narrow spring as illustrated in the schematic view of FIG. **1**. The two vertical switches of FIG. **2** include first and second plates. Inductors may be one turn as illustrated in FIG. **2** or multi-turn as illustrated in FIGS. **15***a* and **15***b*. FIG. **15***a* illustrates an exemplary embodiment of a planar spiral multi-turn inductor. FIG. **15***b* illustrates an exemplary embodiment of an out-of-plane solenoid inductor. Springs are designed to have a small series resistance and stiffness. The actuation voltage of the vertical switch with an actuation gap of 3.8 μm is 40 V. This voltage can be reduced to less than 5 V by reducing the gap size to ~0.9 μm. A close-up view of the switch showing the actuation gap is shown in FIG. **3**.

Fabrication

A schematic diagram illustrating the process flow of an exemplary fabrication method **30** for producing an exemplary inductor **10** is shown in FIGS. **4***a-h*. A substrate **11** is provided **31**. The substrate **11** is spin-coated **32** with a thick low-loss dielectric **12** such as polymer **12** (20 μm in this case), such as Avatrel™ (available from Promerus, LLC, Brecksville, Ohio), for example. A routing metal layer **14** is formed **33** by evaporating a thick silver layer **14** (2 μm in this case), for example. A thin adhesion layer **13** (~100 A°) such as titanium (Ti), for example, may be used to promote the adhesion between the routing metal layer **14** (silver layer **14**) and the polymer layer **12**. An actuation gap **20** is then defined by depositing **34** a layer of plasma enhanced chemical vapor deposited (PECVD) sacrificial silicon dioxide layer **15** at 160° C. (3.8 μm thick in this case). The deposition temperature of silicon dioxide layer **15** was reduced to preserve the quality of the polymer layer **12**, which provides mechanical support for the released device. Inductors and switches are formed **35** by electroplating silver **17** into a photoresist mold **16** (20 μm thick in this case). A thin layer **18** of Ti/Ag/Ti (100 A°/300 A°/100 A°) is sputter deposited to serve as a seed layer **18** for plating. The top titanium layer of the seed layer **18** prevents the electroplating of silver **17** underneath the electroplating mold **16**, and may be dry etched from open areas in a reactive ion etching system (RIE). The use of the titanium layer is important when the distance between the silver lines is less than 10 μm.

An exemplary plating bath consists of 0.35 mol/L of potassium silver cyanide (KAgCN) and 1.69 mol/L of potassium cyanide (KCN). A current density of 1 mA/cm^2 may be used in the plating process. The electroplating mold **16** is subsequently removed **36**. The seed layer **18** may be removed **37** using a combination of wet and dry etching processes. Compared to sputtered silver, the electroplated silver layer **17** has a larger grain size resulting in a higher wet etch rate using an

H_2O_2:NH_4OH solution. The hydrogen peroxide oxidizes the silver and the ammonium hydroxide solution complexes and dissolves the silver ions. When wet etched, the thick high-aspect ratio lines of electroplated silver **17** etch much faster than the sputtered seed layer **18** that is between the walls of thick electroplated silver **17**. Dry etching silver on the other hand, decouples the oxidation and dissolution steps resulting in almost the same removal rate for the small-grained sputtered layer **18** as the large-grained plated silver **17**. The silver is first oxidized in an oxygen plasma (dry etch) and then the resultant silver oxide layer is dissolved in dilute ammonium hydroxide solution. Using this etching method, the seed layer **18** is removed **37** without losing excess electroplated silver **17**. The device **10** is then released **38** in dilute hydrofluoric acid.

The released device **10** is then wafer-level packaged **41-43** (FIGS. **4***e*-**4***g*). This may be done as disclosed by P. Monajemi, et al., in "A low-cost wafer-level packaging technology," *IEEE International Conference on Microelectromechanical Systems*, Miami, Fla. January 2005, pp. 634-637, for example. A thermally-decomposable sacrificial polymer **21**, Unity® (available from Promerus LLC, Brecksville, Ohio, 44141), is applied and patterned **41** (FIG. **4***e*). Then, the over-coat polymer **22** (Avatrel™), which is thermally stable at the decomposition temperature of the decomposable sacrificial polymer **21**, is spin-coated and patterned **42** (FIG. **4***f*). Finally, the sacrificial polymer **21** is decomposed **43** at 180° C. (FIG. **4***g*). As discussed in the P. Monajemi, et al. paper, the resulting gaseous products diffuse out through a solid Avatrel™ over-coat **22** with no perforations. The loss caused by the silicon substrate **11** may be eliminated, if necessary, by selective backside etching **44** (FIG. **4***h*), to form an optional backside cavity **24**, leaving a polymer membrane **12** under the device **10**. Alternatively, the loss caused by the silicon substrate **11** may be eliminated, if necessary, by selective etching **50** of the substrate before encapsulating the device (FIG. **4***d'*), to form an optional cavity **51** under the device **10**. A micrograph of an un-packaged inductor taken from the backside of the Avatrel™ polymer membrane **12** is shown in FIG. **5**. The highest processing temperature, including the packaging steps, is 180° C. and thus the process is post-CMOS compatible.

Regarding materials that may be employed to fabricate the inductor **10**, the substrate **11** may be silicon, CMOS, BiCMOS, gallium arsenide, indium phosphide, glass, ceramic, silicon carbide, sapphire, organic or polymer. The dielectric layer **12** may be silicon dioxide, silicon nitride, hafnium dioxide, zirconium oxide or low-loss polymer. The conductive layers may be polysilicon, silver, gold, aluminum, nickel or copper.

Simulation Results

The tunable inductors **10** were simulated in the Sonnet electromagnetic tool. FIGS. **6***a* and **6***b* shows the simulated effective inductance and Q seen from port one at four states of the tunable inductor (State (A) is when all the switches are off). As shown in FIG. **6***a*, a maximum inductance change of 47% is expected at the frequency of the peak Q, when both switches are on. At low frequencies, R_i is not negligible compared to $L_i\omega$ and, according to equation (6), the percent tuning is small. At higher frequencies, $L_i\omega \gg R_i$ and magnetic coupling is stronger. Therefore, the amount of tuning increases at higher frequencies. The outer inductor at Port **2** is larger in size than the inner inductor at Port **2**, and its peak Q occurs at lower frequencies. As a result, the outer inductor has a larger effect on the effective inductance at lower frequencies. In contrast, the frequency of the peak Q for the inner inductor is higher. Thus, the inner inductor at Port **2** has a larger effect at this frequency range.

Measurement Results

Several switched tunable inductors **10** were fabricated and tested. On-wafer S-parameter measurements were carried out using an hp 8510C VNA and Cascade GSG microprobes. Pad parasitics were not de-embedded. Each switched tunable inductor **10** was tested several times to ensure repeatability of the measurements.

FIG. **7** shows the measured inductance of a switched silver inductor **10** fabricated on an Avatrel™ polymer membrane **12**. The inductance is switched to four different values and is tuned from 1.1 nH at 6 GHz to 0.54 nH, which represents a maximum tuning of 47% at 6 GHz. The maximum tuning was achieved when both secondary inductors were switched on. At 6 GHz, the effective inductance drops to 0.79 nH when the outer inductor (the larger inductor at Port **2**) is on, and 0.82 nH when the inner inductor (the smaller inductor at port **2**) is on. The measured results are in good agreement with the simulated response as shown in FIGS. **6** and **7**. The measured embedded Q of this inductor **10** in different states is shown in FIG. **8**. As shown, the inductor **10** exhibits a peak Q of 45 when the inductors at port two are both off. The Q drops to 20 when both switches are on. The drop of Q is consistent with Equation (2). When any of the inductors at port two are switched on, L_{eq} decreases while the effective resistance increases resulting in a drop in Q as the inductor **10** is tuned. FIG. **9** shows the measured Q of the inductors at port two. From FIG. **9**, it can be seen that the peak Q of the inner inductor (smaller inductor at port **2**) is at frequencies >7 GHz. Thus, the maximum change in the effective inductance resulting from switching on the inner inductor occurs (smaller inductor at port **2**) at this frequency range (FIG. **7**).

Effect of Q on Tuning

To demonstrate the effect of the quality factor on the tuning ratio of the switched tunable inductors **10**, substantially identical devices were fabricated on different substrates **11**. On sample A, inductors **10** were fabricated on a CMOS-grade silicon substrate **11** passivated with a 20 μm thick PECVD silicon dioxide layer. The silicon substrate **11** was removed from the backside of the primary and secondary inductors of sample B to enhance their Q, leaving behind a 20 μm thick silicon dioxide membrane beneath the inductors. Silicon dioxide has a higher loss tangent than Avatrel™ polymer **12**, which results in a higher substrate loss. Therefore, the Q of inductors on a silicon dioxide membrane (sample B) is lower than that of inductors on an Avatrel™ polymer membrane **12** as shown in FIG. **8**.

FIG. **10** compares the effective inductance and Q of the tunable inductors **10** on samples A and B at two different states. As shown in FIG. **10**, the percent tuning is lower for sample A that has a lower Q. The inductance of sample A changes by 36.8% at 4.7 GHz when the outer inductor is switched on (State A'). At this frequency, the tuning resulting from switching on the outer inductor of sample B (State B') is only 9.7%. Consequently, employing low-loss materials such as Avatrel™ polymer helps improving the tuning characteristic of the switched tunable inductors **10**.

The performance of the tunable inductors **10** may be further improved. The routing metal layer **14** of the fabricated inductors **10** is less than three times the skin depth of silver at low frequencies, where the metal loss is the dominant Q-limiting mechanism. Therefore, the quality factor (Q) of the switched tunable inductors **10** is limited by the metal loss of the routing metal layer **14** and can be improved by increasing the thickness of this layer **14**.

Packaging Results

Hermetic or semi-hermetic sealing of silver microstructures increases the lifetime of the silver devices by decreasing its exposure to the corrosive gases and humidity. Silver is very sensitive to hydrogen sulfide (H_2S), which forms silver sulfide (Ag_2S), even at a very low concentration of corrosive gas. The decomposition of the contact surfaces leads to an increase of the surface resistance, hence, to a lower Q and for tunable inductors a lower tuning range. Another problem that impedes the wide use of silver is electrochemical migration which occurs in the presence of wet surface and applied bias. Silver migration usually occurs between adjacent conductors/electrodes, which leads to the formation of dendrites and finally results in an electrical short-circuit failure. The failure time is related to the relative humidity, temperature, and the strength of the electric field. For the structure of the tunable inductor **10** disclosed herein, a possible location of failure is between the switch pads only when the switch is in contact. When off, there is an air gap between the switch pads which blocks the path for the growth of dendrites.

A semi-hermetic packaging technique may be used to prevent or lower their exposure to the corrosive gases, and to encapsulate the tunable inductor **10**. If necessary, subsequent over-molding can provide additional strength and resilience, and ensures long-term hermeticity. FIG. **11***a* is a SEM view of the packaged switched tunable inductor **10** and a close-up view of a broken package is presented in FIG. **11***b* showing the air cavity **23** inside. The inductor trace was peeled during the cleaving process.

FIG. **12** shows the Q of two identical inductors **10** before decomposition of the sacrificial polymer **21**. The two inductors **10**, one packaged and one un-packaged were fabricated on silicon nitride-passivated high-resistivity (ρ=1 kΩ-cm) silicon substrate **11**. The un-decomposed packaged inductor **10** has a lower Q at higher frequencies because of the dielectric loss of the Unity® sacrificial polymer **21**. When the Unity® sacrificial polymer **21** was decomposed and the packaging process was completed, the two inductors **10** were measured again. As shown in FIG. **13**, the switched tunable inductor **10** showed no degradation in Q after packaging, indicating the Unity® sacrificial polymer **21** was fully decomposed. To demonstrate the effect of packaging on preserving the Q of the silver tunable inductor **10**, the performance of the packaged inductor **10** was measured after ten months and is shown in FIG. **14**. The performance of the packaged inductor **10** did not change during this time period.

Thus, improved microelectromechanical systems (MEMS) switched tunable inductors have been disclosed. It is to be understood that the above-described embodiments are merely illustrative of some of the many specific embodiments that represent applications of the principles discussed above. Clearly, numerous and other arrangements can be readily devised by those skilled in the art without departing from the scope of the invention.

What is claimed is:

1. A microelectromechanical tunable inductor apparatus comprising:
- a substrate;
- a dielectric layer disposed on the substrate;
- a first conductive layer disposed on the dielectric layer;
- a second conductive layer comprising:
  - a primary inductor;
  - a plurality of secondary inductors positioned in proximity to the primary inductor, the plurality of secondary inductors including a first secondary and a second secondary inductors, the primary inductor positioned between the first secondary and second secondary inductors; and
  - a plurality of micromechanical switches coupled to the plurality of secondary inductors, each switch having an actuation air gap, and wherein each switch is switched on and off to change the effective inductance of the primary inductor; and
- an outer protective member that contacts the dielectric layer and encapsulates the inductors and switches inside a cavity.

2. The apparatus recited in claim **1** wherein the substrate is selected from a group including silicon, CMOS, BiCMOS, gallium arsenide, indium phosphide, glass, ceramic, silicon carbide, sapphire, organic and polymer.

3. The apparatus recited in claim **1** wherein the dielectric layer is selected from a group including silicon dioxide, silicon nitride, hafnium dioxide, zirconium oxide and low-loss polymer.

4. The apparatus recited in claim **1** wherein the conductive layers are selected from a group including polysilicon, silver, gold, aluminum, nickel, and copper.

5. The apparatus recited in claim **1** wherein the outer protective member comprises a polymer.

6. The apparatus is claim **1** wherein the primary inductor and the secondary inductors are planar spiral inductors.

7. The apparatus in claim **1** wherein the primary inductor and the secondary inductors are out-of-plane solenoid inductors, wherein the out-of-plane solenoid inductors are not interwound.

8. The apparatus in claim **1** wherein the secondary inductors are multi-turn inductors.

9. The apparatus in claim **1** wherein the substrate comprises a cavity formed under the conductive layers to reduce the substrate loss.

10. The apparatus recited in claim **1** wherein the switches have an electrically isolated actuation port formed using the first conductive layer.

11. A microelectromechanical tunable inductor apparatus comprising:
- a substrate;
- a dielectric layer disposed on the substrate;
- a first conductive layer disposed on the dielectric layer forming a routing for inductors and first plates of a plurality of vertical micromechanical switches;
- a second conductive layer comprising:
  - a primary inductor;
  - a plurality of secondary inductors positioned in proximity to the primary inductor; and
  - second plates of the plurality of vertical micromechanical switches that are coupled to the plurality of secondary inductors by way of suspended conductive springs, each switch having an actuation air gap, and wherein each switch is switched on and off to change the effective inductance of the primary inductor; and
- an outer protective member that contacts the dielectric layer and encapsulates the inductors and switches inside a cavity.

12. The apparatus recited in claim **11** wherein the switches have an electrically isolated actuation port formed using the routing layer.

13. The apparatus recited in claim **1** wherein the switches are coupled to the secondary inductors by way of suspended conductive springs.

14. The apparatus recited in claim **11** wherein the substrate is silicon.

15. The apparatus recited in claim **11** wherein the conductive layers are silver.

16. The apparatus recited in claim **11** wherein the outer protective member comprises a polymer.

17. The apparatus in claim **11** wherein the primary inductor and the secondary inductors are planar spiral inductors.

18. The apparatus in claim **11** wherein the secondary inductors are multi-turn inductors.

19. The apparatus in claim **11** wherein the substrate comprises a cavity formed under the conductive layers to reduce the substrate loss.

20. The apparatus in claim **17**, wherein the primary inductor and the secondary inductors are concentric.

21. The apparatus of claim **11**, wherein the effective inductance of the primary winding depends upon the number of switches that are switched on.

22. The apparatus of claim **11** wherein the primary inductor and secondary inductors are out-of-plane solenoid inductors, wherein the out-of-plane solenoid inductors are not interwound.

* * * * *